BULLETIN OF THE POLISH ACADEMY OF SCIENCES
TECHNICAL SCIENCES, Vol. 68, No. 1, 2020
DOI: 10.24425/bpasts.2020.131838

Large-signal averaged models of the non-ideal flyback converter derived by the separation of variables

W. JANKE, M. BĄCZEK, and J. KRAŚNIEWSKI*

Department of Electronics and Computer Science, Koszalin University of Technology, 2 Śniadeckich St., 75-453 Koszalin, Poland

Abstract. The main topic of the paper is the large signal averaged model of a switch-mode flyback power converter. The use of the large-signal averaged models of switching converters allows for fast simulation of power systems. The known averaged models of a flyback are based on the state-space averaging or switch-averaging approach. The model presented in the paper is derived with the use of the separation of variables approach and include parasitic resistances of all converter components. The limitations of the model accuracy are discussed. The calculations based on the averaged model are compared with detailed full-wave simulations and measurements results.

Key words: switch-mode converter, flyback, averaged models, separation of variables, large-signal simulation.

1. Introduction

Transformer-based converters are an important group of switch-mode DC-DC converters and have unique features: DC isolation between input and output, broad range of the voltage transfer functions, the possibility to generate multiple outputs. The most representative example of the transformer-based converters is a flyback converter. The basic version of a flyback is considered in this paper. The basic properties of a flyback converter are widely described in many sources, including textbooks [1, 2], technical data and application notes. The detailed analysis, modeling for simulation purposes, design methods and propositions of modifications may be found in many papers, for example [3–8].

Averaged modeling is a generally accepted approach to a simplified description of DC-DC converters and is presented not only in numerous papers and application notes but also in textbooks, as for example [1, 2]. Averaged models describe the behavior of switching converter in the low frequency range including frequencies of external signals (changes of input voltage, load current etc.) and the characteristic frequency of a power stage, much smaller than the switching frequency of a converter. Averaged model of the power stage of a switching power converter may be obtained by one of possible approaches: state-space averaging, an averaged switch modeling [1, 2], or the separation of variables [9, 10]. In the procedure of averaged models derivation, a large signal nonlinear averaged model is obtained first and then, a small signal averaged model is derived by the linearization of the large signal model [1, 2].

The knowledge of a small signal averaged model in the form of a proper transmittance (usually, control-to-output transmittance) is necessary in the designing a control system for a power converter. The large-signal averaged model may be used not only for finding small-signal one, but also as a convenient description of a power converter in the fast, simplified time-domain simulation of a power system containing converters.

Averaged models of switching power converters, mainly consisting of simple, transformer-less converters are extensively discussed in many sources. The averaged descriptions of flyback converters presented in the literature usually apply to the idealized converter models in which such effects as the series resistances of the transformer and parasitic resistances of transistors, diodes and capacitors are not included or included only partially, as in [11, 12], while the small-signal version of the models is discussed. In [13] , the averaged modeling of flyback is only mentioned, but the main considerations concern the general model without averaging.

Averaged models of a non-ideal flyback with parasitic resistances of all principal components are considered to the limited extent in the literature, and the most representative example seems to be papers [14] and [15] in which the interesting modifications of the standard state-space averaging and the switch averaging technique, specific for a flyback converter, are introduced, with the parasitic resistances of all converter components included. Some results of the calculations of transients in a converter obtained by presented models are compared with the simulations based on the full-wave description including switching. Unfortunately, the form of the proposed models is inconvenient – the averaged description contains some variables that are defined only for the specific subinterval, so the additional calculations have to be performed. No comparisons of the simulation results with the experiments are presented.

This paper is devoted to the presentation of the large-signal averaged models of a non-ideal flyback converter in the form of the set of equations and equivalent circuits. Apart from the derivation of the models based on the separation of variables principle (Section 2), the examples of their application to the simulation of the large-signal behavior of a converter is shown in Section 3. Experimentally obtained waveforms are compared

*e-mail: jaroslaw.krasniewski@ie.tu.koszalin.pl

Manuscript submitted 2019-09-04, revised 2019-11-08, initially accepted for publication 2019-11-29, published in February 2020

to the calculations based on the averaged models and to the results of simulations taking into account the full waveforms during switching processes. Concluding remarks are given in Section 4.

2. Large-signal averaged models of flyback and their circuit representation

2.1. Introductory remarks. The basic description of the power stage of a non-ideal flyback used in the further considerations is presented in Fig. 1. The ideal part of the transformer is represented by two controlled sources $-n \cdot v_L$ and $-n \cdot i_D$ and so called magnetizing inductance L. The parasitic effects in the transformer are represented by the resistances R_{L1} and R_{L2}. The semiconductor switches are represented as ideal switches $S1$ and $S2$ in series with their parasitic resistances R_T and R_D. The series resistance of the capacitor is R_C. The averaged model of a converter should describe the relations between currents and voltages averaged over single switching period. The parasitic leakage inductances of the transformer and capacitances of semiconductor switches are not included in the derivation of the averaged models, which are valid only for the low frequency range.

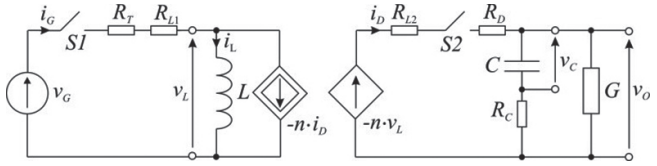

Fig. 1. The power stage of a flyback converter

The difference between two possible modes of the converter operation – continuous conduction (CCM) and discontinuous conduction (DCM) may be observed in Fig. 2, presenting the waveforms of the current i_L in magnetizing inductance in both modes where: T_S – switching period, t_{ON} – time when the ON phase ends, t_X – time when the OFF1 phase ends.

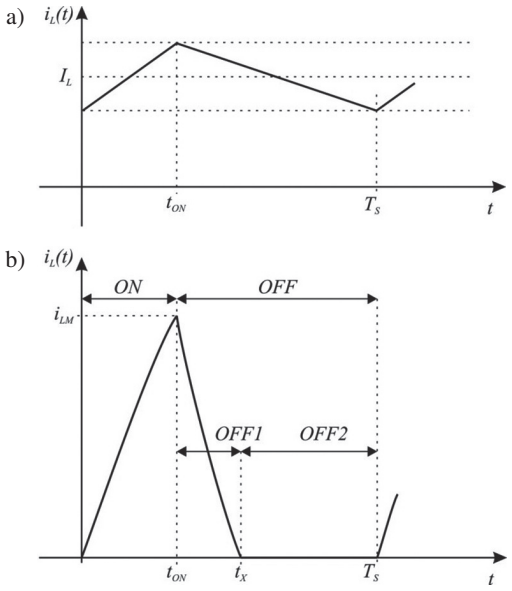

Fig. 2. Waveforms of the current $i_L(t)$ in the magnetizing inductance: a) in CCM; b) in DCM

The calculated waveforms of $i_L(t)$ for an ideal converter in both modes are linear, but in a real converter they are slightly nonlinear because of the parasitic resistances. The deviation from linearity is better visible in DCM because the relative changes of i_L are greater than in CCM. It is illustrated by the shape of $i_L(t)$ dependence in Fig. 2. The averaged models of a non-ideal flyback are considered in subsections 2.2 and 2.3.

2.2. Continuous conduction mode (CCM). A converter in CCM may be described separately in two subintervals: ON ($S1$ ON, $S2$ OFF) and OFF ($S1$ OFF, $S2$ ON). The equivalent circuits for these subintervals, obtained from the model in Fig. 1 are shown in Fig. 3a and 3b, where resistances R_{TL} and R_{DL} are defined as:

$$R_{TL} = R_T + R_{L1}\,, \tag{1}$$

$$R_{DL} = R_D + R_{L2}\,. \tag{2}$$

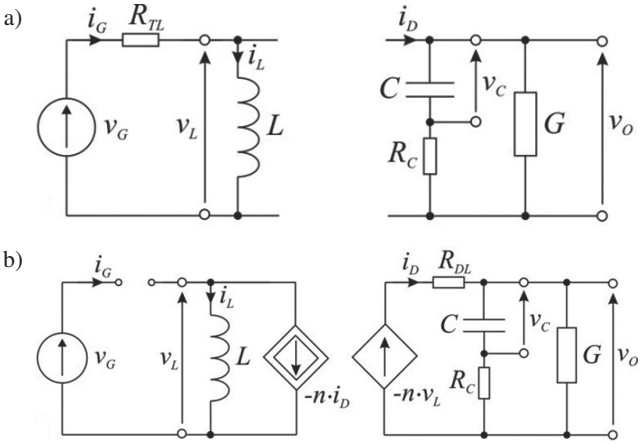

Fig. 3. Equivalent circuits of a non-ideal flyback in CCM: a) ON state; b) OFF state

The set of variables describing a non-ideal flyback converter contains: v_G, v_O, d_A, i_L, i_D, v_C. The part of the equations, true for both subintervals, and also for averaged values, obtained from Fig. 1, is as follows:

$$v_L = L \cdot \frac{\mathrm{d}i_L}{\mathrm{d}t}\,, \tag{3}$$

$$v_O = v_C + R_C \cdot \frac{\mathrm{d}v_C}{\mathrm{d}t}\,, \tag{4}$$

$$i_D = C \cdot \frac{\mathrm{d}v_C}{\mathrm{d}t} + G \cdot v_O\,. \tag{5}$$

For finding other equations for averaged quantities, it is convenient to use the concept of the local average of each circuit variable in given subinterval. According to the separation of variables idea [21], the circuit variables are divided into two

groups. Group A contains variables having the same local averages in subintervals ON and OFF, equal consequently to the averaged values in the whole switching period. Group B contains the variables with different local averages in ON and OFF subintervals. The local averages of the variables of group B are represented as functions of the variables of group A for each subinterval and next the averaging equation is applied:

$$x_{AV} = d_A \cdot x(ON) + (1 - d_A) \cdot x(OFF), \tag{6}$$

where d_A is duty ratio of the switching signal, x_{AV} is average value of the variable x for the whole switching period, $x(ON)$ and $x(OFF)$ are local averages of x in ON and OFF subintervals, respectively. In the case of flyback in CCM, group A consists of variables v_G, v_O and it is assumed that the current i_L may be also treated as a group A quantity, because the time-dependence of i_L is nearly linear (see Fig. 2a). The sufficient set of group B variables is: v_L, i_D and i_G.

For the subinterval ON:

$$v_L(ON) = v_G - R_{TL} \cdot i_L, \tag{7}$$

$$i_D(ON) = 0, \tag{8}$$

$$i_G(ON) = i_L. \tag{9}$$

For the subinterval OFF:

$$i_D(OFF) = \frac{i_L}{n}, \tag{10}$$

$$v_L(OFF) = -\frac{1}{n} \cdot v_O - \frac{i_L}{n^2} \cdot R_{DL}, \tag{11}$$

$$i_G(OFF) = 0. \tag{12}$$

Next, applying Eq. (6) to the variables v_L, i_D, i_G, one obtains the following expressions for averages:

$$v_{LAV} = d_A \cdot v_G - (1 - d_A) \cdot \frac{v_O}{n} - \\ - i_L \cdot \left[d_A \cdot R_{TL} + (1 - d_A) \cdot \frac{R_{DL}}{n^2} \right], \tag{13}$$

$$i_{DAV} = (1 - d_A) \cdot \frac{i_L}{n}, \tag{14}$$

$$i_{GAV} = d_A \cdot i_L. \tag{15}$$

The subscript AV in Eqs. (13)–(15) is applied to the quantities of group B only, because in the case of group A quantities (according to their definition), there is no need to distinguish their averaged values from values in the subinterval ON or OFF. The quantity in the square brackets in (13) may be treated as a duty-controlled resistance $r_{EQ}(d_A)$:

$$r_{EQ}(d_A) = d_A \cdot R_{TL} + (1 - d_A) \cdot \frac{R_{DL}}{n^2}, \tag{16}$$

therefore:

$$v_{LAV} = d_A \cdot v_G - (1 - d_A) \cdot \frac{v_O}{n} - i_L \cdot r_{EQ}(d_A). \tag{17}$$

The voltage drop corresponding to the last terms in (13) and (17) may be alternatively treated as the voltage source controlled by i_L and d_A.

The large-signal averaged model of a non-ideal flyback converter in CCM is expressed by equations (3), (4), (5), (13), (14) and (15) and may be presented in the form of the equivalent circuit shown in Fig. 4a, where the central cell may be replaced by the cell shown in Fig. 4b. Symbol v_X denotes voltage source described as:

$$v_X = i_L \cdot \left[d_A \cdot R_{TL} + (1 - d_A) \cdot \frac{R_{DL}}{n^2} \right]. \tag{18}$$

In the further text and figures of subsection 2.2, only the averaged values of the circuit variables are present, therefore the subscript AV is omitted.

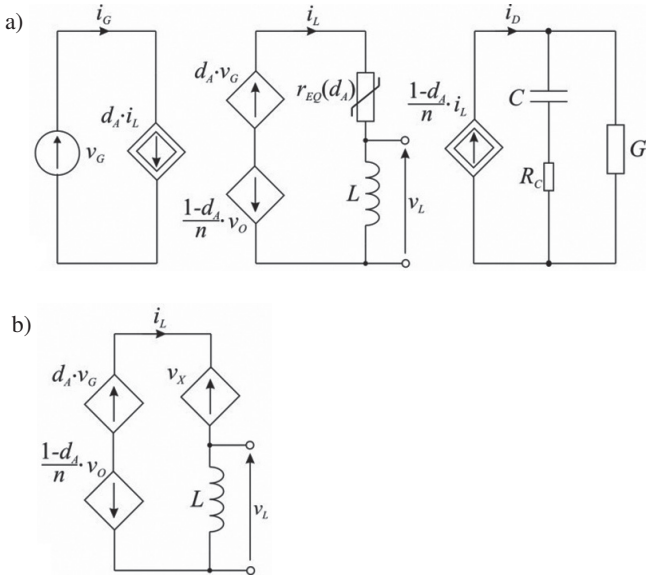

Fig. 4. The equivalent circuit representing the averaged, large-signal model of the non-ideal flyback converter in CCM: a) basic form, b) the alternative form of the central cell

A DC version of the averaged model of the non-ideal flyback in CCM is obtained by setting to zero the inductor voltage and capacitor current in the model shown in Fig. 4. The result is presented in Fig. 5, where the symbols of DC components of variables are applied.

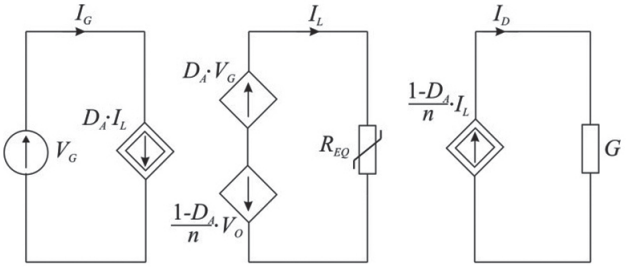

Fig. 5. DC averaged model of flyback in CCM

From Fig. 5 one obtains:

$$D_A \cdot V_G = \frac{1-D_A}{n} \cdot V_O + R_{EQ} \cdot I_L, \tag{19}$$

where:

$$R_{EQ} = D_A \cdot R_{TL} + (1-D_A) \cdot \frac{R_{DL}}{n^2}. \tag{20}$$

In addition:

$$I_L = \frac{n}{1-D_A} \cdot G \cdot V_O \tag{21}$$

and

$$I_G = D_A \cdot I_L = \frac{n \cdot D_A}{1-D_A} \cdot G \cdot V_O. \tag{22}$$

From (19) and (21) one obtains:

$$V_O = \frac{\dfrac{n \cdot D_A}{1-D_A}}{1 + G \cdot R_{EQ} \cdot \dfrac{n^2}{(1-D_A)^2}} \cdot V_G. \tag{23}$$

Therefore, the DC voltage transfer function is:

$$M_V = \frac{M_{Vi}}{1 + G \cdot R_{EQ} \cdot \dfrac{n^2}{(1-D_A)^2}}. \tag{24}$$

The quantity M_{Vi} in (24) denotes the DC voltage transfer function in the ideal case (for $R_{EQ} = 0$):

$$M_{Vi} = \frac{n \cdot D_A}{1-D_A}. \tag{25}$$

From (22) and (25) we have:

$$I_G = M_{Vi} \cdot I_O. \tag{26}$$

Equations (25) and (26), true for an ideal flyback converter in CCM correspond to the known description of a flyback [1, 2]. In the description of a non-ideal flyback in [1], only the parasitic resistance of the transistor is included. In [2], more involved description of a converter is given in which, the impact of the switching losses on the DC voltage transfer is included.

2.3. Discontinuous conduction mode (DCM). A characteristic feature of the DCM is the shape of the current i_L of the inductive element L, shown in Fig. 2b. The sub-period OFF consists of two parts, OFF1 and OFF2 and in the OFF2 state, both semiconductor switches are OFF. The equivalent circuits shown in Figs. 3a and 3b may be used to the description of a converter in DCM in the states ON and OFF1. Equivalent circuit for OFF2 is shown in Fig. 6. Referring to the idea of the separation of variables, the current i_L does not belong to group A of variables in DCM, because its local averages in ON and OFF sub-periods are different. The only variables of group A in DCM are the input and output voltages v_G and v_O.

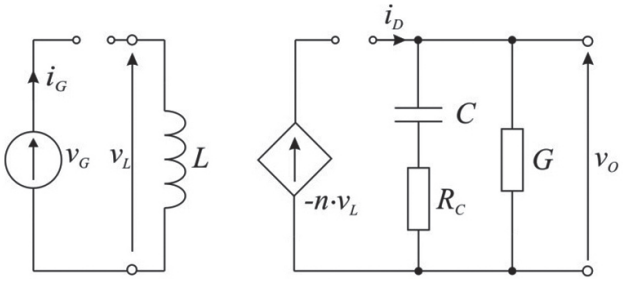

Fig. 6. Equivalent circuit of a flyback in DCM in the OFF2 subinterval

The first step in the derivation of the averaged model of converter in DCM is finding the average value v_{LAV} on the ideal part L of inductive element. From Fig. 2b we have:

$$\begin{aligned} v_{LAV} &= \frac{1}{T_S} \int_0^{T_S} v_L(t)\,\mathrm{d}t \\ &= \frac{1}{T_S} \left(\int_0^{t_{ON}} v_{L1}\,\mathrm{d}t + \int_{t_{ON}}^{t_X} v_{L2}\,\mathrm{d}t + 0 \right), \end{aligned} \tag{27}$$

where:

$$v_{L1}(t) = L \frac{\mathrm{d}i_{L1}}{\mathrm{d}t}, \tag{28}$$

$$v_{L2}(t) = L \frac{\mathrm{d}i_{L2}}{\mathrm{d}t}, \tag{29}$$

$t_{ON} \le t_x < T_S$.

$i_{L1}(t)$ and $i_{L2}(t)$ denote the waveforms of the $i_L(t)$ current in subintervals ON and OFF1 respectively (see Fig. 2b).

From Eqs. (27)–(29) we obtain:

$$v_{LAV} = \frac{L}{T_S} \left(i_{L1}(t_{ON}) - i_{L1}(0) + i_{L2}(t_X) - i_{L2}(t_{ON}) \right) = 0. \tag{30}$$

The result is independent of the particular shape of the $i_{L1}(t)$ and $i_{L2}(t)$ dependencies. It means that the ideal part of the inductive element L is shorted in the averaged model for DCM. For the derivation of the model, the dependencies of the averaged currents i_{GAV} and i_{DAV} on the voltages v_G, v_O and duty ratio d_A should be found. Currents i_G and i_D in each state are directly connected to the current i_L, therefore the description of i_L should be found first. In the ON state, from Fig. 3a, one obtains:

$$v_G = i_{L1} \cdot R_{TL} + L \cdot \frac{\mathrm{d}i_{L1}}{\mathrm{d}t} \tag{31}$$

where:

$$i_{L1}(t) = 0, \quad \text{for } t = 0. \tag{32}$$

The resulting description of $i_{L1}(t)$ is:

$$i_{L1}(t) = \frac{v_G}{R_{TL}} \cdot \left[1 - \exp\left(-\frac{R_{TL}}{L} \cdot t \right) \right], \quad \text{for } 0 \le t \le t_{ON}. \tag{33}$$

In the OFF1 state, for $t_{ON} \le t \le t_X$, from Fig. 3b:

$$-n \cdot L \cdot \frac{\mathrm{d}i_{L2}}{\mathrm{d}t} = \frac{i_L}{n} \cdot R_{DL} + v_O \tag{34}$$

where:

$$i_{L2}(t_{ON}) = i_{L1}(t_{ON}) = i_{LM}. \tag{35}$$

The quantity i_{LM} denoting the maximum value of the current i_L can be calculated by putting $t = t_{ON} = d_A \cdot T_S$ in Eq. (33) and may be approximated by:

$$i_{LM} \cong \frac{v_G}{L} \cdot d_A \cdot T_S. \tag{36}$$

The solution of Eq. (34) is:

$$i_{L2}(t) = -\frac{n \cdot v_O}{R_{DL}} + \left(i_{LM} + \frac{n \cdot v_O}{R_{DL}}\right) \cdot \cdot \exp\left(-\frac{R_{DL}}{n^2 \cdot L} \cdot (t - t_{ON})\right), \text{ for } t_{ON} \le t \le t_X. \tag{37}$$

The current i_L in each state depends on v_G and v_O, i.e. on the quantities belonging to the group A, in accordance to the separation of variables rule.

Current $i_G(t)$ equals $i_{L1}(t)$ in the ON state and is zero in other states. Current $i_D(t)$ equals $i_{L2}(t)/n$ in the OFF1 state and is zero in other states. Consequently, the averages of $i_G(t)$ and $i_D(t)$ are:

$$i_{GAV} = \frac{1}{T_S} \cdot \int_0^{t_{ON}} i_{L1}(t) \cdot \mathrm{d}t = \frac{Q_1}{T_S}, \tag{38}$$

$$i_{DAV} = \frac{1}{T_S} \cdot \frac{1}{n} \cdot \int_{t_{ON}}^{t_X} i_{L2}(t) \cdot \mathrm{d}t = \frac{Q_2}{n \cdot T_S}. \tag{39}$$

Q_1 and Q_2 denote the respective integrals of currents i_{L1} and i_{L2}. From Eq. (33) we obtain:

$$Q_1 = \frac{v_G}{R_{TL}} \cdot \left[t_{ON} + \frac{L}{R_{TL}} \cdot \left(\exp\left(-\frac{R_{TL}}{L} \cdot t_{ON}\right) - 1\right)\right]. \tag{40}$$

Using the approximation:

$$e^x \cong 1 + x + \frac{x^2}{2} \tag{41}$$

one obtains:

$$Q_1 \cong \frac{v_G}{2 \cdot L} \cdot t_{ON}^2 = \frac{v_G}{2 \cdot L} \cdot d_A^2 \cdot T_S^2. \tag{42}$$

From (37) we have:

$$Q_2 = -\frac{n \cdot v_O}{R_{DL}} \cdot (t_X - t_{ON}) + + \left(\frac{v_G}{L} \cdot t_{ON} + \frac{n \cdot v_O}{R_{DL}}\right) \cdot \left(\frac{n^2 \cdot L}{R_{DL}}\right) \cdot \cdot \left[1 - \exp\left(-\frac{R_{DL}}{n^2 \cdot L} \cdot (t_X - t_{ON})\right)\right]. \tag{43}$$

Using the approximation (41) we obtain:

$$Q_2 \cong \frac{(t_X - t_{ON})}{L} \cdot \cdot \left[v_G \cdot d_A \cdot T_S - \frac{(t_X - t_{ON})}{2 \cdot n} \cdot \cdot \left(v_O + \frac{v_G \cdot R_{DL} \cdot d_A \cdot T_S}{n \cdot L}\right)\right]. \tag{44}$$

The time point t_X (denoting the end of the OFF1 subinterval) is defined by the condition $i_{L2}(t_X) = 0$, that leads to:

$$t_X = t_{ON} + \frac{n^2 \cdot L}{R_{DL}} \cdot \ln\left(1 + \frac{R_{DL} \cdot i_{LM}}{n \cdot v_O}\right). \tag{45}$$

The averaged quantities i_{GAV} and i_{DAV} described by Eqs. (38) and (39), with the expressions (40) and (43), or their approximations (42) and (44), depend on the input and output voltages v_G and v_O and on duty ratio d_A.

The resulting large-signal averaged model of a non-ideal flyback in DCM may be presented in the form of equivalent circuit shown in Fig. 7a. The subscript AV in the description of the circuit in Fig. 7 is omitted, because the dependencies concern only the averaged quantities. The description of the controlled sources $i_G(v_G, d_A)$ and $i_D(v_G, v_O, d_A)$ based on the approximations (42) and (44) are:

$$i_G = f_1(v_G, d_A) = \frac{v_G}{2 \cdot L} \cdot d_A^2 \cdot T_S \tag{46}$$

and

$$i_D = f_2(d_A, v_G, v_O) = \frac{t_X - t_{ON}}{n} \cdot \cdot \left[d_A \cdot v_G - \frac{t_X - t_{ON}}{2 \cdot n \cdot T_S} \cdot \left(v_O + \frac{v_G \cdot R_{DL} \cdot d_A \cdot T_S}{n \cdot L}\right)\right]. \tag{47}$$

Using additionally the approximation $\ln(1+x) \cong x$ in (45) we can obtain a simplified expression for the current i_D:

$$i_D \cong \frac{d_A^2 \cdot T_S \cdot v_G^2}{2 \cdot L \cdot v_O} \cdot \left(1 - \frac{v_G \cdot R_{DL} \cdot d_A \cdot T_S}{v_O \cdot n \cdot L}\right). \tag{48}$$

The controlled current source in the input cell in Fig. 7a may be treated as the duty-controlled conductance as shown in Fig. 7b.

The DC version of the averaged model for DCM mode is obtained by setting to zero the capacitor current. From the DC averaged model, the static voltage transfer function may be calculated, because DC component of i_D (dependent on Q_2) is equal to the load current, $I_O = G \cdot V_O$. The quantity Q_2, according to Eqs. (43) or (44), together with Eq. (45) depends on the voltages v_G and v_O, therefore the dependence between v_G and v_O may be found. Unfortunately, even with the use of approximate equation (44) for Q_2, the expression for v_O cannot be found in the analytical form. It may be shown however, that after neglecting the parasitic resistance R_{DL} in equations (44) and (45) one obtains the ideal formula for the static voltage transfer function,

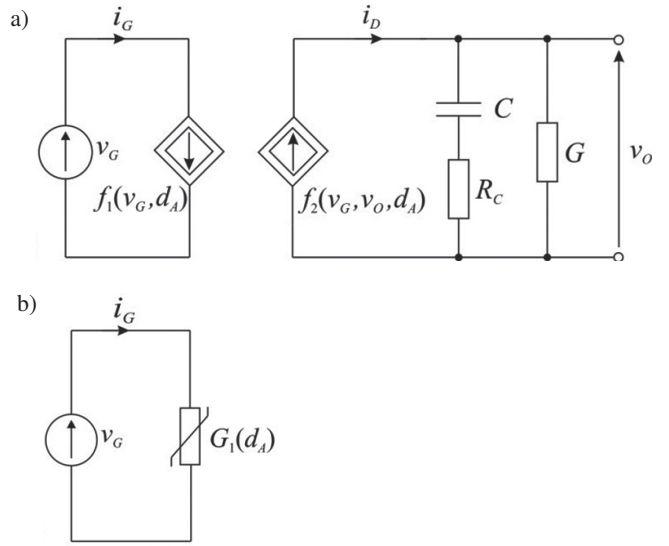

Fig. 7. Large signal averaged model of a non-ideal flyback converter in DCM: a) basic form, b) the current source in the input cell replaced by the duty-controlled conductance

consistent with equations given in [1] and [2]:

$$M_{VDi} = D_A \cdot \sqrt{\frac{T_S}{2 \cdot L \cdot G}}. \tag{49}$$

3. Simulations and measurements

In real flyback converters, the waveforms of currents and voltages within each switching period resulting from switching processes in semiconductor components and the resonances caused by parasitic capacitances and inductances are observed, as in the example shown in Fig. 8. The accurate simulation of such waveforms demands the use of very complex models of the converter elements and, consequently, is time-consuming. On the other hand, the changes of external signals (input voltage, load current) for converter working in more complex power system as well as changes resulting from the internal time constants of a converter are relatively slow. The fast, approximate simulations of a converter for time segments containing hundreds or thousands switching periods may be performed with the use of large-signal averaged models. The usability of models presented in the previous section to such simulations may be evaluated on the examples presented below.

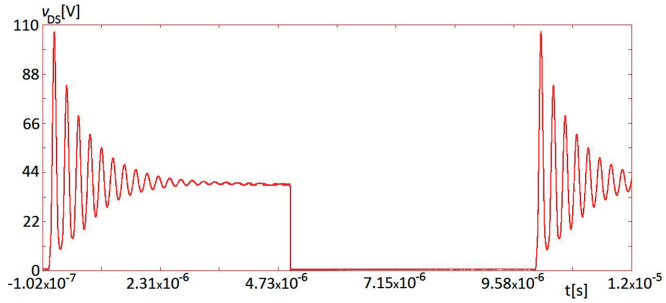

Fig. 8. The waveforms of the voltage v_{DS} on the switch $S1$ in CCM

Figures 9–11 show the waveforms of the output voltage of the converter for a step change of the input voltage or the duty ratio, obtained by the averaged models, full-wave simulations or measurements. Main circuit parameters are: $f_S = 100$ kHz; $n = 0.2$; $L = 150$ µH; $C = 570$ µF. Load resistance is 3.3 Ω for CCM and 50 Ω for DCM. The waveforms in Fig. 9 are obtained for $d_A = 0.5$ and the input voltage step 0–20 V; the waveforms in Fig. 10 – for $d_A = 0.3$ and input voltage step 0–24 V. Fig. 11 corresponds to step change of d_A: 0.3 to 0.2 at constant input voltage 24 V. Curves 1 represent results of full-wave simulations; 2 – simulations based on the averaged model; 3 – measurements. Other data for simulations based on the averaged model are: $R_{L1} = 0.5$ Ω; $R_{L2} = 23$ mΩ; $R_T = 163$ mΩ; $R_D = 100$ mΩ; $R_C = 53$ mΩ. In the full-wave simulations transistor and diode are represented by the Spice library models of

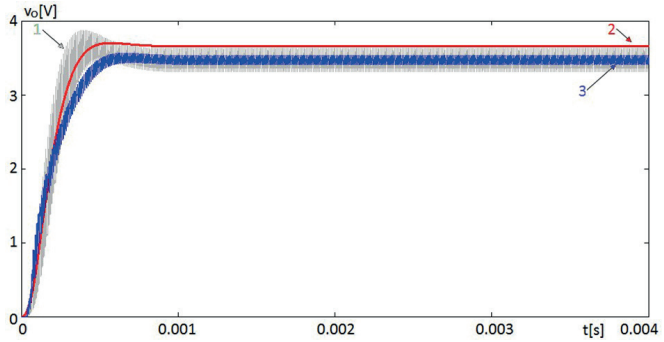

Fig. 9. The output voltage response to the input voltage step in CCM

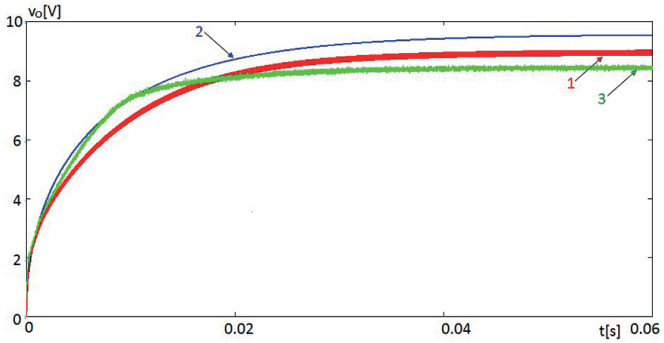

Fig. 10. The output voltage response to the input voltage step in DCM

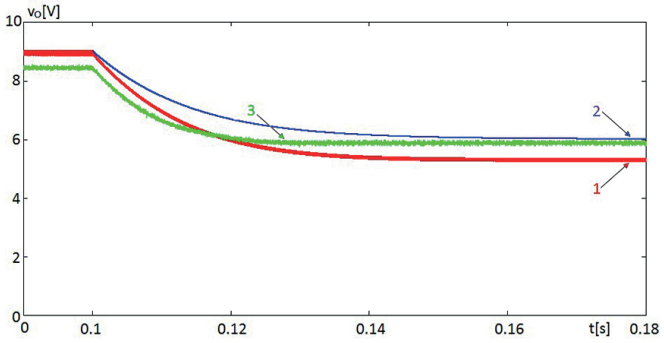

Fig. 11. The output voltage response to the step change of the duty ratio in DCM

the devices TPH3206 and MBR1035. In addition, leakage inductances of the primary and secondary coils of transformer $L_{RP} = 1.5$ µH, $L_{RS} = 1$ nH are taken into account in full-wave simulations. The values of resistances R_T and R_D are obtained from the measured DC characteristics of the transistor and diode. The values of other parasitic parameters are extracted from measurements of the impedances of capacitor and input and output coils of transformer. In particular, the leakage inductance L_{RP} has been measured for shorted transformer output and L_{RS} – for shorted transformer input.

The differences between the waveforms obtained by two variants of simulation and measurements, which may be observed in Figs. 9–11, are the result of the fact, that each model may represent the real object only approximately. In particular, the averaged model doesn't include high frequency phenomena, connected to switching processes and, by definition, is the approximation.

The waveforms of the output voltage for more complex changes of the input voltage (0–20–30–40 V) at $d_A = 0.5$ shown in Fig. 12, and duty ratio d_A (0.4–0.6–0.8) at $v_G = 20$ V shown in Fig. 13 are obtained by full-wave simulations (curve 1) and on the base of the averaged model (curves 2) for switching frequency $f_S = 200$ kHz and changed capacitor parameters: $C = 470$ µF, $R_C = 76$ mΩ. The differences between waveforms obtained by the accurate full-wave simulations and approximate simulations based on the averaged model are relatively small but the differences in the simulation time in Spice are gigantic

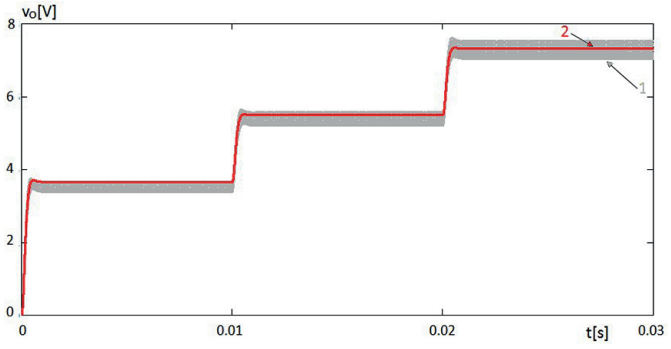

Fig. 12. The output voltage response to the step change of the input voltage in CCM

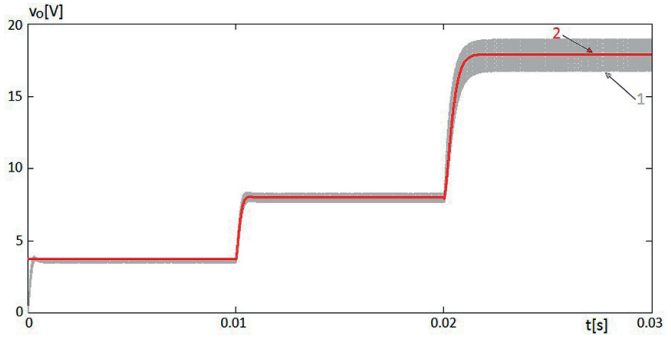

Fig. 13. The output voltage response to the step change of the duty ratio in CCM

(averaged models: 20 ms in both cases; full-wave: 1123.97 s or 1287.75 s). This comparison shows the main advantage of using averaged instead of full-wave approach for large-signal, time domain simulations of power systems containing converters.

4. Conclusions

The large-signal averaged models of switching power converters are usually used as a first step for finding small-signal averaged models needed in the designing process of control subcircuits. On the other hand, large signal averaged models may serve as a convenient tool for performing fast, approximate simulations of power systems. The averaged models of flyback known so far are based on the state-space averaging or switch averaging approach and usually take the parasitic resistances of the converter components into account only partially [11, 12] or have an inconvenient form as in [14] and [15]. The models presented in this paper are derived for the continuous conduction mode (CCM) and discontinuous conduction mode (DCM) with the use of the separation of variables and include the parasitic resistances of the all components of a converter. The final form of the models may be directly implemented in large signal time domain circuit simulators. The exemplary calculations based on the presented averaged models are compared with the detailed full-wave simulations and the measurements results and a relatively good consistency is observed. The main advantage of the use of averaged models in large-signal power system simulations is the simulation speed.

References

[1] R.W. Erickson and D. Maksimovic, *Fundamentals of Power Electronics*, 2-nd Edition, Kluwer, 2002.

[2] M.K. Kazimierczuk, *Pulse-Width Modulated DC–DC Power Converters*, J. Wiley, 2008.

[3] W. Fa-Quiang and M. Xi-Ku, "Effects of Switching Frequency and Leakage Inductance on Slow-Scale Stability in a Voltage Controlled Flyback Converter", *Chin. Phys. B* 22 (12) (2013), 120504-1–120504-8.

[4] E. Wang, "Feedback Control Design of Off-line Flyback Converter", Richtek Technology Corporation, Application Note AN017, Jun 2014.

[5] P.C. Chao, W.D. Chen, and R.H. Wu, "A Battery Charge Controller Realized by a Flyback Converter with Digital Primary Side Regulation for Mobile Phones", *Microsyst.Technol.* (2014).

[6] S.K. Pandey, S.L. Patti, and V.S. Rajguru, "Isolated Flyback Converter, Designing, Modeling and Suitable Control Strategies", Int. Conf. on Advances in Power Electronics and Instrumentation Engineering, 2014.

[7] N. Kasundra and A. Kumar, "Design and Simulation of Flyback Converter in MATLAB using PID Controller", *International Journal of Advanced Research in Electrical, Electronics and Instrumentation Engineering* 5 (2), 960–965 (2016).

[8] N.S. Jayalaksami, D.N. Gaonkar, and A. Naik, "Design and Analysis of Dual Output Flyback Converter for Standalone PV/Battery System", *International Journal of Renewable Energy Research* 7 (3), 1032–1040 (2017).

[9] W. Janke, "Averaged Models of Pulse-Modulated DC-DC Converters, Part II. Models Based on the Separation of Variables", *Archives of Electrical Engineering* 61 (4), 633–654 (2012).

[10] W. Janke, "Equivalent Circuits for Averaged Description of DC-DC Switch-Mode Power Converters Based on Separation of Variables Approach", *Bull. Pol. Ac.: Tech.* 61 (3), 711–723 (2013).

[11] A.S. Raj, A.M. Siddeshwar, K.P. Guruswamy Maheshan, and V.C. Sanekere, "Modelling of flyback converter using state space averaging technique", Computing and Communication Technologies (CONECCT), IEEE International Conference on Electronics, 2015.

[12] S. Xu, Q. Qian, B. Ren, and Q. Liu, "An Accurate Small Signal Modeling and Control Loop Design of Active Clamp Flyback Converter", 10th Int. Conf. On Power Electronics – ECCE Asia, Korea, 2019.

[13] G. Gatto, A. Lai, I. Marongiu, and A. Seppi, "Circuital and Mathematical Modelling of Flyback Converters", Int. Symp. On Power Electronics, Electrical Drives, Automation and Motion, 2016, 906–911.

[14] S.A. Akbarabadi, H. Atighechi, and J. Jatskevich, "Corrected State-Space Averaged-Value Modeling of Second-Order Flyback Converter Including Conduction Losses", 26th IEEE Canadian Conference of Electrical and Computer Engineering, Canada, 2013.

[15] S.A. Akbarabadi, H. Atighechi, and J. Jatskevich, "Circuit-Averaged and State-Space-Averaged-Value Modeling of Second-Order Flyback Converter in CCM and DCM Including Conduction Losses", 4th International Conference on Power Engineering, Energy and Electrical Drivers, Istanbul, 2013, 995–1000.